Level Set Methods for Modeling Air-Water-Grain Interactions at the Microscale

Christopher E. Kees[1], Jason H. Collins[2], and Tristan de Lataillade[1]
[1]U.S. Army Coastal and Hydraulics Laboratory, Vicksburg, MS; [2] US Army Corps of Engineers, New Orleans District

Introduction

We seek to understand micro-scale momentum exchange among fluids and granular solids (e.g. air, water, and sand). The long-term research program is to inform coastal and riverine sediment transport modeling at practical engineering scales, with micromechanical simulations. To this end, we have developed a computational laboratory that can simulate two-phase fluid flow and rigid particle interactions across regimes and processes characterizing important engineering applications. To resolve these processes at the grain scale requires development of numerical methods that are robust and accurate through topological changes in the air, water, and solid phase distributions. These changes occur frequently due to changing granular contacts and fluid saturation distributions. This work presents several new techniques under investigation to improve the accuracy and robustness of the existing framework.

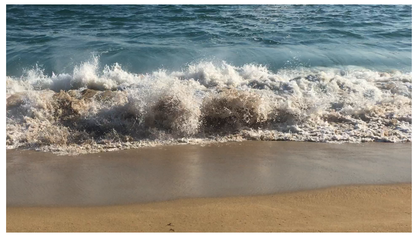

Figure 1: Surf zone wave breaking and erosion processes.

Background

- To model air and water, including surface tension effects, coupled with solid grain dynamics, including solid contacts, we need to model two dynamic interfaces: the fluid-fluid (air-water) interface, Γ_f, and the fluid-solid interface, Γ_s as shown in Figure 2.
- Due to changing inter-granular contacts and bubble/droplet formation, the model formulation or numerical method must handle topological change of the phase subdomains,$\Omega_s, \Omega_w, \Omega_a$, robustly and accurately.
- In this work we extend the level set method presented in [6] to address the challenge of topological change in fluid-fluid-solid simulation numerically, leading to the definition of scalar functions ϕ_s and ϕ_f with the following properties:

$$\Omega_s(t) = \{\mathbf{x} \in \Omega | \phi_s(x,t) < 0\} \tag{1a}$$
$$\Omega_w(t) = \{\mathbf{x} \in \Omega | \phi_f(x,t) < 0\} \tag{1b}$$
$$\Omega_a(t) = \{\mathbf{x} \in \Omega | \phi_f(x,t) > 0\} \tag{1c}$$
$$\Gamma_s(t) = \{\mathbf{x} \in \Omega | \phi_s(x,t) = 0\} \tag{1d}$$
$$\Gamma_f(t) = \{\mathbf{x} \in \Omega | \phi_f(x,t) = 0\} \tag{1e}$$

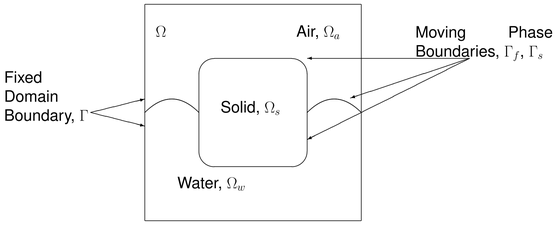

Figure 2: The fixed computational domain Ω and boundary Γ, with three dynamic subdomains Ω_w, Ω_a, and Ω_s and phase boundaries Γ_f and Γ_s

Prior Work in Proteus and Chrono

In prior work, we have developed a numerical laboratory combining Finite Element Methods (FEMs) from Proteus (https://proteustoolkit.org), and Discrete Element Methods (DEMs) from Chrono (https://projectchrono.org). The approach is based generally on level set methods, while using regularized Heaviside and Dirac functions to approximate volume and surface integrals on cells cut by the interface. These methods can produce qualitatively correct results for problems involving granular contacts and surface tension [11, 10]. Also of note is the recently proposed Level Set DEM method [5], which supports direct calculation of solid phase dynamics from imagery while using a level set description consistent with the approach in Proteus for fluids.

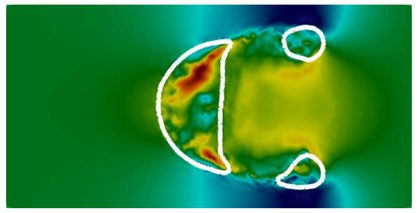

Figure 3: Bubble dynamics using the level set method and an approximation of the Laplace-Beltrami operator to model surface tension.

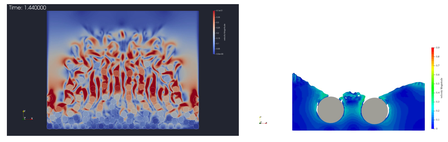

Figure 4: Grain dynamics in water and air/water flows based on regularized Heaviside and Dirac distributions to enforce fluid-solid coupling.

Challenges

Our prior work has uncovered several issues with the unfitted level set approach for both air/water and air/water/solid applications, specifically:

- Strong mesh sensitivity of critical integral quantities, such as the drag and torque on particles shown in Figure 4.
- Difficulty resolving thin jets and related shear layers.
- Inability to preserve certain equilibrium states, such as flat water surface at hydrostatic pressure and zero velocity (lake at rest).

These issues arise from the use of regularized Heaviside and Dirac functions to approximate integrals in cells cut by interfacial boundaries, which reduces accuracy of the method to $\mathcal{O}(h)$. We seek to replace these integrals with exact computations and precise enforcement of interfacial jump conditions.

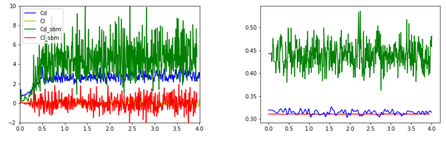

Figure 5: Force (drag) and surface area due to various unfitted representations.

Primitive Formulation

$$\nabla \cdot \mathbf{u}_a = 0, \qquad \text{in } \Omega_a \tag{2a}$$
$$\rho_a(\partial_t \mathbf{u}_a + (\mathbf{u}_a \cdot \nabla)\mathbf{u}_a) - \nabla \cdot \sigma_a = \rho_a \mathbf{g}, \qquad \text{in } \Omega_a \tag{2b}$$
$$\nabla \cdot \mathbf{u}_w = 0, \qquad \text{in } \Omega_w \tag{2c}$$
$$\rho_w(\partial_t \mathbf{u}_w + (\mathbf{u}_w \cdot \nabla)\mathbf{u}_w) - \nabla \cdot \sigma_w = \rho_w \mathbf{g}, \qquad \text{in } \Omega_w \tag{2d}$$
$$\mathbf{u}_a - \mathbf{u}_w = 0 \qquad \text{on } \Gamma_f \tag{2e}$$
$$\sigma_a \cdot \mathbf{n}_f - \sigma_w \cdot \mathbf{n}_f = \gamma \kappa \mathbf{n}_f \qquad \text{on } \Gamma_f \tag{2f}$$
$$\sigma_a \cdot \mathbf{t}_{1,f} - \sigma_w \cdot \mathbf{t}_{1,f} = 0 \qquad \text{on } \Gamma_f \tag{2g}$$
$$\sigma_a \cdot \mathbf{t}_{2,f} - \sigma_w \cdot \mathbf{t}_{2,f} = 0 \qquad \text{on } \Gamma_f \tag{2h}$$
$$\mathbf{u} - \mathbf{u}_s = \mathbf{u}_c \qquad \text{on } \Gamma_s \tag{2i}$$
$$\mathbf{u} \cdot \mathbf{n} = 0 \qquad \text{on } \Gamma \tag{2j}$$

where

$$\sigma = -pI + 2\mu\varepsilon(\mathbf{u}) \tag{3}$$

is the Cauchy stress tensor for an incompressible, Newtonian fluid, and

$$\varepsilon(\mathbf{u}) = \frac{1}{2}\left(\nabla \mathbf{u} + \nabla \mathbf{u}^T\right) \tag{4}$$

is the symmetric gradient. Gravitational accelerations is $\mathbf{g}$, and the material properties are the densities, ρ_a, ρ_w, viscosities μ_a, μ_w, and surface tension constant γ. Note: this model allows for a jump in the normal component of fluid stresses at the air/water interface due to surface tension and slip velocity $\mathbf{u}_c$ due to contact line dynamics.

Nitsche's Method and CutFEM

Nitsche developed an approach to approximately enforcing Dirichlet conditions that for an elliptic equation leads to the weak formulation: Find $u_h in V_h(\Omega)$ such that

$$a_h(u_h, w_h) = \langle f, w \rangle \quad \forall w_h \in V_h(\Omega) \tag{5}$$

where

$$V_h(\Omega) = \left\{ v \in C^0(\Omega) : v|_K \in P^1(K), \quad \forall K \in \mathcal{T}_h \right\} \tag{6}$$

and

$$a_h(u_h, w_h) = \int_{\Omega_f} \mu \nabla u_h \cdot \nabla w_h + \tag{7}$$
$$\int_{\Gamma_s} -\mu \nabla u_h \cdot \mathbf{n} w_h - \mu \nabla w_h \cdot \mathbf{n} u_h + \frac{C}{h} u_h w_h \tag{8}$$
$$< f, w_h > = \int_{\Omega_f} f w_h - \int_{\Gamma_s} \mu \nabla w_h u_s + \int_{\Gamma_s} \frac{C}{h} u_s w_h \tag{9}$$

where C is a numerical parameter. This formulation provides a precise (discretely conservative) numerical flux at the boundary and retains the underlying symmetry of the problem.

Nitsche's method was originally applied in the context of immersed boundary methods in [2]. A key idea of this approach is to locate "cut" cells of the triangulation K such that $K \cap \Gamma_f \neq \emptyset$ and $K = K_a \cap K_w$ where $K_a = \Omega_a \cap K$ and $K_w = \Omega_w \cap k$ and use the local basis on K twice (i.e. double the number of degrees of freedom on K), associating one set of basis functions with K_a and one with K_w. Then Nitsche's method can be applied over the boundary cut Γ_K separating the polygonal cells K_a and K_w. For the embedded solid grain boundaries, the natural extension of the CutFEM approach [1]

In the CutFEM approach for embedded solids, a "ghost penalty" must be added to prevent loss of coercivity and bound the matrix condition number independently of the location of the cuts, Γ_k. This term is critical for moving solids and unstructured meshes, as Figure 6 demonstrates for a simple flow through an embedded duct.

$$j(u_h, v_h) := \sum_{F \in \mathcal{F}_G} \int_F [\gamma(\nabla u^+ - \nabla u^-) \cdot \mathbf{n}][(\nabla w^+ - \nabla w^-) \cdot \mathbf{n})] dS \tag{10}$$

where $\mathcal{F}_G$ is the set of internal element boundaries of cut cells.

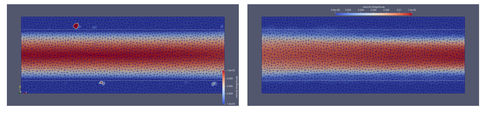

Figure 6: CutFEM without ghost penalty (left) and with ghost penalty (right).

Immersed Interface Method (IFEM)

For two-fluid immersed interface problems, Leveque and Li developed a second order accurate finite difference scheme for by enforcing jump conditions for the solution and normal derivatives across the interface [7, 8]. This approach was extended to FEM in the Immersed Finite Element Method (IFEM), by constructing a local basis with the desired jump conditions[9]. A key insight is that the algebraic system that results from doubling the number of degrees of freedom (as in CutFEM) leads to a solvable algebraic system for exactly half the duplicated degrees of freedom. Consider and elliptic immersed boundary problem with homogeneous jump conditions.

$$[u] = 0 \qquad [\mu \nabla u \cdot \mathbf{n}_f] = 0 \qquad \text{on } \Gamma_f \tag{11}$$

To illustrate construction of the modified basis on cut elements, consider one dimension where the cut element K is $(x_0, x_1) = (0, 1)$, $\Gamma_f = x_c \in (0, 1)$, and $\mathbf{n_f} = 1$. Define a new basis, ψ_0, ψ_1 on K by

$$\psi_i = \begin{cases} \psi_i^a = a_1 + a_2 x & x \leq x_c \\ \psi_i^w = b_1 + b_2 x & x > x_c \end{cases} \tag{12}$$
$$\psi_i^a(x_0) = \delta_{i0} \tag{13}$$
$$\psi_i^b(x_1) = \delta_{i1} \tag{14}$$
$$\psi_i^a(x_c) = \psi_i^b(x_c) \tag{15}$$
$$\mu_a \nabla \psi_i^b \cdot \mathbf{n}_f = \mu_w \nabla \psi_i^b \cdot \mathbf{n}_f \tag{16}$$

Constraints 13-16 are a system of four linear equations in the unknowns a_1, a_2, b_1, b_2. The solution for $\mu_a = 1, \mu_w = 2$ is shown in Figure 7 below, where the standard linear basis functions are (black) and modified IFEM basis functions are (solid red/blue).

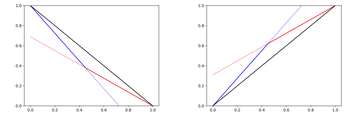

(Figure 7.)

For the linear basis functions on simplicial cells, the number of additional coefficients and constraints continue to match as the dimension increases, and the linear system is non-singular [9]. The two-dimensional basis functions are shown in Figure 8.

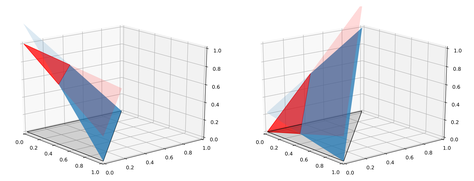

Figure 8: IFEM basis functions (solid red/blue) for $\mu_w/\mu_a = 2$.

In two dimensions and higher the local element basis results in a non-conforming finite element method as global continuity is lost along the simplex boundaries (away from the nodes) as can be seen in Figure 8. It has been shown that methods based on this non-conforming basis, with the addition of an cell boundary penalty term, yields a symmetric, non-conforming scheme with optimal convergence in L^1, L^2, and L^∞ [4].

Cut Cell Integration by Equivalent Polynomials

CutFEM and IFEM introduce cut cells, which are challenge to integrate. After the phase boundaries move, new cell and/or boundary integrals must be computed. If the geometry is based on piecewise linear level sets, then one can locate the linear cuts and generate a sub-triangulation on the fly. An alternative approach described by Ventura and Benvenuti [12], and a closely related to technique for quadrature rules by Holdych and Noble [3], makes use of equivalent polynomial surrogates to the exact Heaviside and Dirac distributions. The key insight is that in finite element methods the integrands that arise are often polynomials with known maximum degree. Integration of cut cells and boundaries using the equivalent polynomials is exact up to the maximum polynomial degree of the integrand. As an example consider a triangular cell K with integrand $f \in P^m(K)$ cut by linear interface $\Gamma = \{x \in K : \phi_h(x) = 0\}$. Define the equivalent polynomial Heaviside $\hat{H}(\phi_h(x)) \in P^m(K)$ as

$$\int_K \hat{H} v_i = \int_K H v_i \quad i = 1, \ldots, \dim(P^m(K)) \tag{17}$$

where $\hat{H}$ is also a polynomial of degree m. Straightforward manipulations lead to equivalent polynomials for the Dirac function, $\delta(\phi)$. For triangular cells cut by piecewise linear level sets, all cut cells and boundaries can then be integrated exactly with standard quadrature of order $2m$.

Future Work

- Determine parallel scaling and performance characteristics of the 3D numerical laboratory.
- Incorporate the full set of jump conditions for Navier-Stokes into the IFEM implementation.
- Develop a modeling approach for contact line dynamics.

References

[1] Burman, E., S. Claus, P. Hansbo, M. G. Larson, and A. Massing, 2015: CutFEM: Discretizing geometry and partial differential equations. *International Journal for Numerical Methods in Engineering*, **104**, 472–501, doi:10.1002/nme.4823.

[2] Hansbo, A. and P. Hansbo, 2002: An unfitted finite element method, based on NitscheÕs method, for elliptic interface problems. *Comput. Methods Appl. Mech. Engrg.*, 16.

[3] Holdych, D. J., D. R. Noble, and R. B. Secor, 2008: Quadrature rules for triangular and tetrahedral elements with generalized functions. *International Journal for Numerical Methods in Engineering*, **73**, 1310–1327, doi:10.1002/nme.2123.

[4] Ji, H., J. Chen, and Z. Li, 2014: A Symmetric and Consistent Immersed Finite Element Method for Interface Problems. *Journal of Scientific Computing*, **61**, 533–557, doi:10.1007/s10915-014-9837-x.

[5] Kawamoto, R., E. Andò, G. Viggiani, and J. E. Andrade, 2016: Level set discrete element method for three-dimensional computations with triaxial case study. *Journal of the Mechanics and Physics of Solids*, **91**, 1–13, doi:10.1016/j.jmps.2016.02.021.

[6] Kees, C. E., I. Akkerman, M. W. Farthing, and Y. Bazilevs, 2011: A conservative level set method suitable for variable-order approximations and unstructured meshes. *Journal of Computational Physics*, **230**, 4536–4558, doi:10.1016/j.jcp.2011.02.030.

[7] LeVeque, R. J. and Z. Li, 1994: The Immersed Interface Method for Elliptic Equations with Discontinuous Coefficients and Singular Sources. *SIAM Journal on Numerical Analysis*, **31**, 1019–1044, doi:10.1137/0731054.

[8] — 1997: Immersed Interface Methods for Stokes Flow with Elastic Boundaries or Surface Tension. *SIAM Journal on Scientific Computing*, **18**, 709–735, doi:10.1137/S1064827595282532.

[9] Li, Z., T. Lin, and X. Wu, 2003: New Cartesian grid methods for interface problems using the finite element formulation. *Numerische Mathematik*, **96**, 61–98, doi:10.1007/s00211-003-0473-x.

[10] Quezada de Luna, M., J. H. Collins, and C. E. Kees, 2019: An unstructured finite element model for incompressible two-phase flow based on a monolithic conservative level set method. *arXiv:1903.06919 [math]*.

[11] Quezada de Luna, M., D. Kuzmin, and C. E. Kees, 2019: A monolithic conservative level set method with built-in redistancing. *Journal of Computational Physics*, **379**, 262–278, doi:10.1016/j.jcp.2018.11.044.

[12] Ventura, G. and E. Benvenuti, 2015: Equivalent polynomials for quadrature in Heaviside function enriched elements. *International Journal for Numerical Methods in Engineering*, **102**, 688–710, doi:10.1002/nme.4679.